

Flexural strengths and fibre efficiency of steel-fibre-reinforced, roller-compacted, polymer modified concrete

Karadelis, J. and Yougui, Lin

Pre-print deposited in [Curve](#) June 2015

Original citation:

Karadelis, J. and Yougui, Lin (2015) Flexural strengths and fibre efficiency of steel-fibre-reinforced, roller-compacted, polymer modified concrete. Construction and Building Materials, volume 93 (September): 498-505. DOI: 10.1016/j.conbuildmat.2015.04.059

[Http://dx.doi.org/10.1016/j.conbuildmat.2015.04.059](http://dx.doi.org/10.1016/j.conbuildmat.2015.04.059)

Publisher:

Elsevier

Copyright © and Moral Rights are retained by the author(s) and/ or other copyright owners. A copy can be downloaded for personal non-commercial research or study, without prior permission or charge. This item cannot be reproduced or quoted extensively from without first obtaining permission in writing from the copyright holder(s). The content must not be changed in any way or sold commercially in any format or medium without the formal permission of the copyright holders.

CURVE is the Institutional Repository for Coventry University

<http://curve.coventry.ac.uk/open>

Manuscript Number: CONBUILDMAT-D-14-02087R1

Title: Flexural Strengths and Fibre Efficiency of Steel-Fibre-Reinforced, Roller-Compacted, Polymer Modified Concrete

Article Type: Research Paper

Keywords: steel fibre-reinforced, roller-compacted, polymer-modified, concrete, fibre efficiency

Corresponding Author: Dr. JOHN NICHOLAS KARADELIS, PhD

Corresponding Author's Institution: Coventry University

First Author: JOHN NICHOLAS KARADELIS, PhD

Order of Authors: JOHN NICHOLAS KARADELIS, PhD; Yougui Lin, BSc, MSc, PhD

Abstract: A new material suitable for the structural repair of concrete pavements has been developed at Coventry University exhibiting high flexural, shear and bond strengths and high resistance to reflection cracking, demonstrating also unique 'placeability' and 'compactability' properties. This article deals with the standard equivalent flexural strengths evaluated using the identical fibre bridging concept and the size effect. Correlation of flexural strengths for beams of different sizes was achieved and the efficiency of fibre in the mix was scrutinised. It was concluded that the efficiency was much higher in the new steel-fibre reinforced, roller compacted, polymer modified concrete (SFR-RC-PMC) mix than in conventional concrete. The high efficiency revealed by the fibre bridging law is mainly attributed to a lower water to cement ratio. It was also found that the fibre aspect ratio influences significantly the flexural performance of the new material. The very high flexural strength extracted from the SFR-RC-PMC, compared to conventional steel-fibre reinforced concrete is very favourable to worn concrete pavement rehabilitation.

Dear Editor

Manuscript Number: CONBUILDMAT-D-14-02087

Title: Flexural Strengths and Fibre Efficiency of Steel-Fibre-Reinforced, Roller-Compacted, Polymer Modified Concrete

Please accept the revised submission of our article with the above title. Revisions were made in accordance with the reviewers' requirements
A Data in Brief article has also been prepared and submitted.

Dr. Yougui Lin is a research assistant at the Department of Civil Engineering Architecture and Building, Faculty of Engineering and Computing, of Coventry University, UK.

Dr. John N Karadelis is senior lecturer, at the Department of Civil Engineering Architecture and Building, Faculty of Engineering and Computing, Coventry University, UK.

Kind regards

John Karadelis and Yougui Lin
28 March 2015

LIST OF CHANGES

Manuscript Number: CONBUILDMAT-D-14-02087

Title: Flexural Strengths and Fibre Efficiency of Steel-Fibre-Reinforced, Roller-Compacted, Polymer Modified Concrete

Article Type: Research Paper

Corresponding Author: Dr. JOHN NICHOLAS KARADELIS, PhD

Corresponding Author's Institution: Coventry University

First Author: JOHN NICHOLAS KARADELIS, PhD

Order of Authors: JOHN NICHOLAS KARADELIS, PhD; Yougui Lin, BSc, MSc, PhD.

	Reviewer's Comments	Author's Response
1	What is the reason for the sharp decrement in flexural strength of PVAPMC in Figure 3?	<p>The reason for the sharp drop of flexural strength of mix PAVPMC1.5%-35 shown in Fig.3 is due to the fact that it exhibited lower flexural toughness than the other mixes. The mix contained 1.5% 35mm-length steel fibre by volume. The flexural performance of the same mix under 3PB shown in Fig.4 also exhibited the same tendency.</p> <p>The article has been amended accordingly (p:5, below Figure 3)</p>
2	In Table 8, how can we use the fibre bridging law in site applications?	<p>The fibre bridging law can serve as an index to evaluate the fibre efficiency for the selection of ingredients during the mix design process in practical (site) applications.</p> <p>For example, mixes SBRPMC1.5%-35 and SBRPMC1.5%-50, in Table 8, are the same (have identical proportions of ingredients), only the former incorporates shorter fibres than the latter. It is apparent from Figure 6 (b) that SBRPMC1.5%-50 is more efficient than SBRPMC1.5%-35 because the fibres of mix -50 provide higher tensile strength than those of -35, for the same crack opening displacement. In this case, the fibre bridging law specified in Table 8, can be used to predict the flexural performance of beams made of the three different mixes.</p> <p>This has been mentioned in the article (p:15, just above the Concluding Remarks)</p>

Flexural Strengths and Fibre Efficiency of Steel-Fibre-Reinforced, Roller-Compacted, Polymer Modified Concrete.

John N Karadelis*, Yougui Lin

Department of Civil Engineering Architecture and Building, Faculty of Engineering and Computing, Coventry University,
Coventry, W. Midlands, CV1 5FB, UK

HIGHLIGHTS:

- Standard equivalent flexural strengths are established for overlay pavement design
- SBRPMC1.5%-35 mix is optimal for flexural and bond strengths and workability
- Lower w/c is the main reason for superior performance of fibre in the SFR-RC-PMC
- The fibre bridging law can be an index of fibre efficiency in a mix design
- The fibre bridging law can be used to predict the flexural performance of beams

Flexural Strengths and Fibre Efficiency of Steel-Fibre-Reinforced, Roller-Compacted, Polymer Modified Concrete.

John N Karadelis*, Yougui Lin

Department of Civil Engineering Architecture and Building, Faculty of Engineering and Computing, Coventry University,
Coventry, W. Midlands, CV1 5FB, UK

Abstract: A new material suitable for the structural repair of concrete pavements has been developed at Coventry University exhibiting high flexural, shear and bond strengths and high resistance to reflection cracking, demonstrating also unique *placeability* and *compactability* properties.

This article deals with the *standard* equivalent flexural strengths evaluated using the *identical fibre bridging concept* and the size effect. Correlation of flexural strengths for beams of different sizes was achieved and the efficiency of fibre in the mix was scrutinised. It was concluded that the efficiency was much higher in the new steel-fibre reinforced, roller compacted, polymer modified concrete (SFR-RC-PMC) mix than in conventional concrete. The high efficiency revealed by the fibre bridging law is mainly attributed to a lower water to cement ratio. It was also found that the fibre aspect ratio influences significantly the flexural performance of the new material. The very high flexural strength extracted from the SFR-RC-PMC, compared to conventional steel-fibre reinforced concrete is very favourable to worn concrete pavement rehabilitation.

Keywords: steel fibre-reinforced, roller-compacted, polymer-modified, concrete, fibre efficiency.

1. Introduction.

Part of the ‘Green Overlays’ research lead by the authors for the last four years involved the development of special concrete mixes used as overlay material, fully bonded on worn concrete pavements. This material exhibits high flexural, shear and bond strengths and high resistance to reflection cracking. It also demonstrates unique *placeability* and *compactability* properties, hence it can be placed on the damaged surface by an asphalt paver and compacted by a vibrating roller [1]. The mixes were named steel-fibre-reinforced, roller-compacted, polymer modified concrete (SFR-RC-PMC). The steel fibre in the mix retards and contains reflective cracking, the polymers enhance its strength and achieve good bond with the old

32 concrete and the roller compaction ensures quick construction. These types of mixes were
33 different from conventional roller-compacted concrete (RCC). Specifically, the optimal water
34 content of the former determined by the modified-light (M-L) compaction method proposed
35 by the authors [1] was usually around 17kg higher than the latter, designed by the modified
36 Vebe method [2 - 3] for 1m³ of concrete, for the same mix proportion [1].

37 Flexural strengths of conventional steel fibre reinforced concrete (SFRC) have been
38 investigated since the 1980s [4 - 11]. A vast amount of literature deals with flexural strength,
39 residual flexural strength, toughness, toughness indexes, crack development and propagation,
40 fibre bridging law, fracture energy, and so on. Neocleous et al. [12 - 13] investigated the
41 flexural performance of steel fibre-reinforced RCC for pavements, while the steel fibres were
42 recovered from used tyres, whereas the mix was conventional RCC. Kagaya et al. [14]
43 investigated the mix design method for steel fibre reinforced RCC pavements by employing
44 the modified Proctor compaction method.

45 It is seen that the mechanical properties of SFR-RC-PMCs have not been investigated to date.
46 In addition, steel fibres in these types of mixes may exhibit a different behaviour to those in
47 conventional SFRCs, due to the fact that the former contains much less cement paste than the
48 conventional concrete, and roller compaction may result in deformation of steel fibres.
49 Furthermore, the flexural performance of PVA (Polyvinyl Alcohol) modified concrete has
50 rarely been investigated. Therefore, it is crucial to investigate the flexural performance of
51 SFR-RC-PMC for overlay pavement design. This article aims to reveal the flexural
52 performance, especially the equivalent flexural strengths of SFR-RC-PMC for overlay
53 pavement design and the efficiency of fibres in RCC.

54

55 **2. Mix Proportion and Specimen Preparation**

56

57 The ingredient materials used (apart from the 50mm-long fibre) were presented in ref. [1] in
58 detail. The 50mm-long fibre was the hooked-end type, with an aspect ratio of 80. The test
59 beams of eight mixes are tabulated in Table 1. Two types of polymers, i.e. SBR (Styrene
60 Butadiene Rubber) and PVA (Polyvinyl Alcohol) and two types of steel fibre, i.e. 35 mm-
61 long and 50 mm-long were used. Super-plasticizer was added in the PVA modified concrete
62 to reduce water content and obtain high strength, while the SBR modified concrete did not
63 incorporate any admixtures. Among a total of eight mixes, five mixes, SBRPMC1%-35,
64 SBRPMC1.5%-35, SBRPMC2%-35, PVAPMC1.5% and SBRPMC1.5%-50 (final numbers
65 of mix ID indicate length of fibres), were SFR-RC-PMC, whose water contents were
66 determined using the M-L compaction method [1]. Mix SBRPMC0%, did not contain fibre
67 and was used as the matrix of mixes SBRPMC1.5%-35 and SBRPMC1.5%-50. Also, it was
68 purposely used for the evaluation of the relative toughness of the same mixes. All beams of
69 the six mixes were fabricated in steel moulds using the vibrating compactor shown in Figure 1,
70 which was purposely designed for specimen formation. The dimensions of the beams of the
71 six mixes were 80 (W) x 100 (H) x 500 (L) mm
72 The mixing procedure can be found in ref. [1]. The mix compaction was carried out in two
73 layers. Each layer was about 40 - 50 mm thick. The vibrating compaction lasted 30 - 50
74 seconds per layer for SBRPMC, and 60 - 90 seconds for PVAPMC until mortar formed a ring
75 around the perimeter of the moulds. The surface of each layer was roughened before
76 accepting the next layer of material. The specimens were de-moulded in twenty-four hours.
77 The SBR modified concrete specimens were cured in water for five days whereas the PVA
78 specimens for seven days, followed by air curing until the test day. The ages of the specimens
79 for tests were 28 days – 40 days.
80 The conventional SFRC, i.e. Con.SBRPMC1.5%-35, was intended for comparison with the
81 mix SBRPMC1.5%-35 to reveal the efficiency of fibres. The former had the same ingredients
82 and mix proportion as the latter except for the water content. The mix Con.SBRPMC0% acted

83 as the matrix of mix Con.SBRPMC1.5%-35. The slump of the mix Con.SBRPMC1.5%-35
 84 was 130 mm. The dimensions of the beams of both mixes were 100 (W) x 100 (H) x 500 (L)
 85 mm, fabricated in steel moulds on the vibrating table. The mixing and curing procedures of
 86 both mixes were the same as for mix SBRPMC1.5%-35.

87

88 **Table 1**

89 Proportion of mixes with optimal water content determined by M-L method (Cem.= Cement, Supe.=
 90 Superplasticizer, Ad.water= Added water)

Mix ID	Mix proportion							Fibre by volume	Wet densi. (Kg/m ³)
	Cem.	Aggr.	Sand	SBR	PVA	Supe.	Ad.water		
SBRPMC1%-35	1	1.266	1.266	0.217	0	0	0.072	1%	2479
SBRPMC1.5%-35	1	1.266	1.266	0.217	0	0	0.095	1.50%	2482
SBRPMC2%-35	1	1.266	1.266	0.217	0	0	0.103	2%	2499
PVAPMC1.5%-35	1	1.266	1.266	0	0.02	0.025	0.228	1.50%	2466
Con.SBRPMC1.5%-35	1	1.266	1.266	0.217	0	0	0.245	1.50%	
SBRPMC1.5%-50	1	1.266	1.266	0.217	0	0	0.095	1.50%	2482
Con.SBRPMC0%	1	1.266	1.266	0.217	0	0	0.245	0%	
SBRPMC0%	1	1.266	1.266	0.217	0	0	0.095	0%	

91



(a) (b)

Figure 1. (a) Vibrating compactor. (b) Steel plate for compaction.

92

93

94

95

96 The beam dimensions recommended by BS [15] are 150 (W) x 150 (H) x 550 (L) mm. The
97 beams used in this study were 80 (W) x 100 (H) x 500 (L), recommended by ASTM [16]. The
98 notches were saw cut to the specified depth by a circular saw one day prior to testing. The
99 width of the notches was 3.5 - 4 mm, complying with BS [15].

100

101 **3. Flexural Strength of PMC Beams**

102

103 **3.1 Strength under four-point bending (4PB) and three-point bending (3PB)**

104

105 The representative test methods for steel fibre reinforced concrete currently available are the
106 ASTM [16] and BS [15] methods. The intact beams of the three mixes, SBRPMC1.5%-35,
107 PVAPMC1.5%-35 and Con.SBRPMC1.5%-35, were tested using four point bending (4PB)
108 arrangements. The loading configuration and experimental setups are shown in Figure 2 (a) &
109 (b). The test procedure complied with ASTM [16]. Two LVDTs measuring net deflection
110 were mounted on both sides of the frame. A hydraulic servo-closed loop test facility with a
111 maximum load capacity of 150 KN was used. The loading rate was controlled by a LVDT
112 placed at mid-span. The representative mid-span deflection was the average of the two LVDT
113 readings. The rate of increase of net deflection was 0.0017 mm/s until the LVDT reading
114 reached 0.5 mm; after the 0.5 mm were reached the rate was increased to 0.0033 mm/s. This
115 is within the range specified by ASTM [16]. The load and vertical displacements were
116 continuously recorded at a frequency of 5Hz. The maximum flexural strength, f_p , and the
117 residual flexural strengths, $f_{R,0.5}$ and $f_{R,2}$ were calculated using eqn.(1) in accordance with
118 ASTM [16]:

119

$$120 \quad f_j = \frac{300P_j}{Bh^2} \quad (1)$$

121

122 Where: $j = P$ (for peak), or $j = R, 0.5$, or $j = R, 2$.

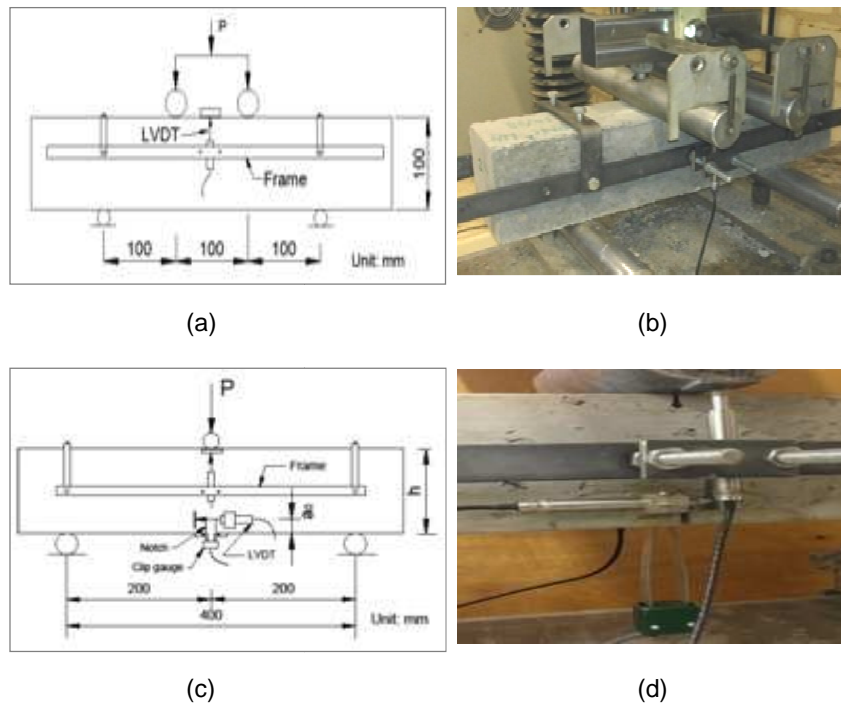
123 In this case, R denotes residual flexural strength. P_p , is the maximum load. $P_{p,0.5}$ is the load
124 corresponding to mid-span deflection equal to 0.5 mm. $P_{p,2}$, is the load corresponding to mid-
125 span deflection equal to 2 mm. f_p , is the maximum flexural strength. $f_{R,0.5}$ and $f_{R,2}$ are strengths
126 corresponding to mid-span deflections of 0.5 and 2 mm respectively. B and h are the breadth
127 and depth of the beam.

128

129 The relationships of flexural strength vs. mid-span deflection for the three mixes are presented
130 in Figure 3. The mid-span deflection was recorded and averaged by two LVDT readings. The
131 laboratory tests showed that all the SBRPMC1.5%-35 and PVAPMC1.5%-35 beams failed
132 with multiple cracking under the 4PB test. However, for concrete used as an overlay on worn
133 concrete pavements, a single reflective crack will initiate from the location of an underlying
134 existing crack of the worn pavement. Therefore, the 3PB test arrangement was chosen as
135 more suitable for concrete overlays.

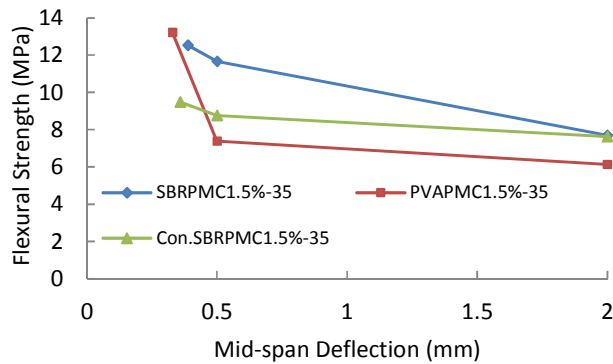
136

137
138



139
140

141 **Figure 2.** (a) Un-notched beam under 4PB. (b) Experimental setup of 4PB test.
142
143 (c) Notched beam under 3PB. (d) Close view of clip gauge and LVDTs mounted on the beam under 3PB.



144
145
146

145 **Figure 3.** Flexural strengths of un-notched beams for three different mixes under 4PB.

147 The reason for the sharp drop of the flexural strength of mix PVAPMC1.5%-35 shown in
148 Figure 3 is due to the fact that it exhibited lower flexural toughness than the other two mixes.
149 The flexural performance of the same mix under a 3PB test, shown in Figure 4, shows also
150 the same tendency. The mix contained 1.5%-35mm length steel fibre by volume.

151 The three-point bending (3PB) test, recommended by BS [15], was employed to measure the
152 flexural performance. The experimental setup is shown in Figure 2, (c) & (d). Six mixes
153 shown in Figure 4 were tested under 3PB complying with the BS [15]. The beams measured
154 80 (W) x 100 (H) x 500 (L) mm, spanning 400 mm with a mid-span notch of 20 mm depth.
155 They were loaded at mid-span. It should be pointed out that the dimensions of the beams used
156 in this study were different from those proposed by BS [15], which are 150 (W) x 150 (H) x
157 550 (L) mm, with span of 500 mm, centrally loaded and notched to the depth of 25 mm.
158 The loading machine was the same as the one used in the 4PB test. One LVDT was fixed on
159 the frame for measuring mid-span (point-load) deflection. The other, for measuring notch tip
160 opening displacement (CTOD), was secured on the beam surface, while the clip gauge was
161 mounted on the underside to measure the crack mouth opening displacement (CMOD) and
162 control the loading rate. Test data were automatically recorded by a computer at the frequency
163 of 5 Hz. The loading rate procedure, controlled by CMOD, was as follows: 0.0001 mm/s until
164 CMOD reached 0.2 mm; 0.0033 mm/s until CMOD reached 3 mm; then 0.005 mm/s until
165 failure of the specimen. The rate of increase CMOD used was much lower than that proposed
166 in the BS [15], which is 0.00083 mm/s until CMOD= 0.1 mm; after that 0.0033 mm/s. All
167 tests were accurately controlled; no abrupt failures occurred and suitable load-CMOD, load-
168 CTOD, and load - load point deflection curves were obtained. These results were used to
169 evaluate the maximum flexural strength, residual flexural strength, equivalent flexural
170 strength, relative toughness index, and total fracture energy and size effects.

171 The flexural strengths were evaluated according to BS [15], using eqns. (2) – (4):

172

$$173 \quad f_{ct,L}^f = \frac{3SP_L}{2Bh_{sp}^2} \quad (2)$$

$$174 \quad f_{R,j} = \frac{3SP_j}{2Bh_{sp}^2} \quad (3)$$

175
$$f_P = \frac{3SP_P}{2Bh_{sp}^2} \quad (4)$$

176 Where: $f_{ct,L}^f$ is the limit of proportionality (LOP) in MPa. P_L is the load corresponding to LOP
177 (N). S is the span (mm). B is the breadth (width) of the specimen (mm). h is the depth (height)
178 of the beam (mm). a_0 is the depth of notch (mm). h_{sp} is the distance between the tip of the
179 notch and the top of the specimen (mm). $f_{R,j}$ is the residual flexural tensile strength. CMOD= j ,
180 $j= 0.5, 1.5, 2.5, \& 3.5$ mm, respectively. P_j is the load corresponding to CMOD= j , (N); f_P is the
181 maximum flexural tensile strength (MPa). P_P is the peak load (N).

182

183 The flexural strength-CMOD relationships are plotted in Figure 4. The compressive strengths
184 of blocks saw-cut from the tested beams are listed in

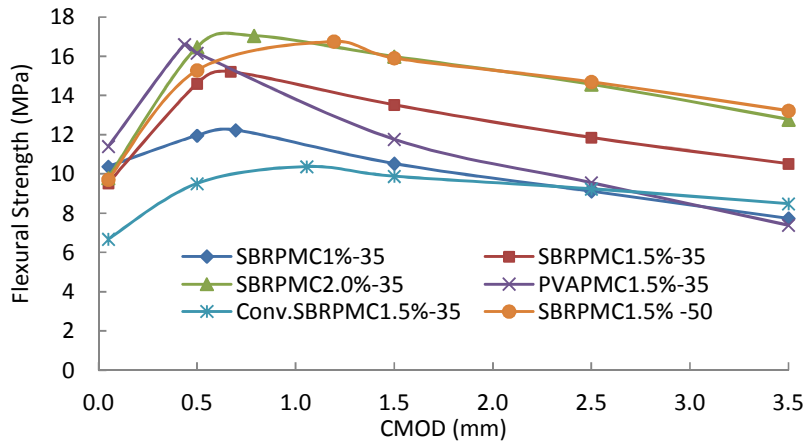
185 Table 2, while the interfacial fracture toughness and splitting tensile bond strength of composite
186 specimens are shown in Table 3. The details for testing interfacial fracture toughness can be
187 found in ref. [17]. It is seen that:

188 a. Compared to conventional SFRC, SFR-RC-PMC exhibited very high flexural
189 strengths, which are desired for worn concrete pavement rehabilitation;

190 b. Compared to the strengths measured under 4PB for the same mix, the obtained
191 strengths under 3PB are remarkably higher.

192 However, the flexural strengths cannot be directly used for overlay pavement design. The
193 design method for SFRC pavements proposed by Altoubat et al [18], requires the flexural
194 strengths to be converted into equivalent flexural strengths.

195



196
197 **Figure 4.** Flexural strengths of six 20mm-notched PMC beams under 3PB
198

199 **Table 2**

200 Compressive strengths of blocks saw-cut from tested beams

Mix ID	Num. of block	Compres. strength (MPa)	
		Average	STDEV
SBRPMC 1%-35	3	83.91	6.69
SBRPMC 1.5%-35	4	79.61	1.48
SBRPMC 2%-35	3	84.76	0.27
Con. SBRPMC 1.5%-35	8	68.18	2.82
PVAPMC 1.5%-35	6	105.87	3.78

201
202
203
204
205
206
207
208
209
210
211

212 **Table 3**

213 Mechanical properties of interface of SBRPMC1.5%-35, PVAPMC1.5%-35 and OPCC to OPCC composite
214 specimens.

Interfacial fracture toughness (J/m ²)	SBRPMC1.5%-35 on-OPCC	Roughened interface	52.0
		Smooth interface	22.6
Splitting tensile bond strength (MPa)	SBRPMC1.5%-35 on-OPCC	Roughened interface	2.96
		Smooth interface	1.8
	PVAPMC1.5%-35 on-OPCC	Roughened interface	3.7
		OPCC-on-OPCC	Roughened interface

215

216 **3.2 Size Effect on Flexural Strength**

217

218 There are two major approaches to explaining the effect of size on the strength of a material:
219 the statistical and deterministic approaches. A representative statistical approach is Weibull's
220 theory [19], while the classic deterministic approach is by Bazant [20 - 21], based on fracture
221 mechanics. According to Weibull's theory [19], a larger specimen has a weaker strength
222 because it has a higher probability of having larger and more severe flaws or defects in it.
223 Table 4, Figures 3 & 4 indicate that for the same mix, the measured flexural strength under
224 4PB is higher than that under 3PB. The reason for this can be explained by Weibull's theory.
225 As has been presented earlier, the tested beams in this study were of dimensions 80 (W) x 100
226 (H) x 400 (S) mm. The beams for 3PB were saw-cut a central notch of 20 mm prior to testing,
227 while the beams for 4PB were intact. In order to use the equivalent concept (presented later),
228 proposed by the Japan Society of Civil Engineers (JSCE-SF4) [22], the flexural strength
229 obtained using 3PB test has to be converted to that by 4PB test.

230 It is seen from Figure 4 that the flexural strength-CMOD curves for all mixes are basically
231 parallel to each other except for the mix PVAPMC1.5%-35. This indicates that all mixes have

232 the same scale factor for equivalent strength conversion. The conversion factor (β_I) can be
233 taken as the ratio of maximum flexural strength under 3PB to that under 4PB. It is used for
234 converting the strength of the small volume to the large volume, which can be explained by
235 Weibull's theory [19].

236 The maximum flexural strengths tested under the 3PB and 4PB are listed in Table 4. The
237 conversion factor, β_I can be easily obtained by simply comparing the f_p in the 4PB to the 3PB,
238 using eqn. (5). The calculated β_I is listed in Table 4.

239

$$240 \quad \beta_1 = \frac{f_p \text{ (in 4PB)}}{f_p \text{ (in 3PB)}} \quad (5)$$

241

242 In this study [23], the flexural strength affected by the height of beams was experimentally
243 investigated. For this purpose, the SBRPMC1.5%-35 beams with the dimensions of 80 (W) x
244 100 (H) x 400 (S) mm and 100 (W) x 150 (H) x 500 (S) mm and with different notch lengths,
245 were tested under 3PB to investigate the size effect on maximum flexural strengths. The size
246 effect law proposed by Bazant [21] was employed. The splitting tensile strength taken from
247 three cylinders with the dimensions $\Phi 100 \times 170$ mm was 9.88 MPa. Consequently, the size
248 effect law obtained using regression analysis for maximum flexural strength of mix
249 SBRPMC1.5%-35 is [23]:

250

$$251 \quad f_p = \frac{80.42}{\sqrt{\frac{h_{sp}}{2.7} - 1}} \quad (6)$$

252 Where: f_p is the maximum flexural strength (MPa). h_{sp} is as per Eqns. (3) & (4).

253 Eqn. (6) will be used to determine the standard equivalent flexural strength later.

254

255 3.3 Equivalent Flexural Strength.

256

257 Altoubat et al. [18] tested an actual size SFRC slab on an elastic foundation, and related the
258 load carrying capacity to the equivalent flexural strength proposed by the Japan Society of
259 Civil Engineers (JSCE-SF4) [22]. He then proposed a simple design method for SFRC
260 pavements. The equivalent flexural strength, $f_{e,3}$ proposed by JSCE-SF4 [22] was measured by
261 conducting a 4PB test. The test beam was 150 (W) x 150 (H) x 450 (S) mm. The equivalent
262 flexural strength was calculated using the area enveloped by load-central deflection curve, and
263 is evaluated by eqn. (7).

264

$$265 \quad f_{e,3} = \frac{S \cdot A_{3mm}}{2Bh^2} \quad (7)$$

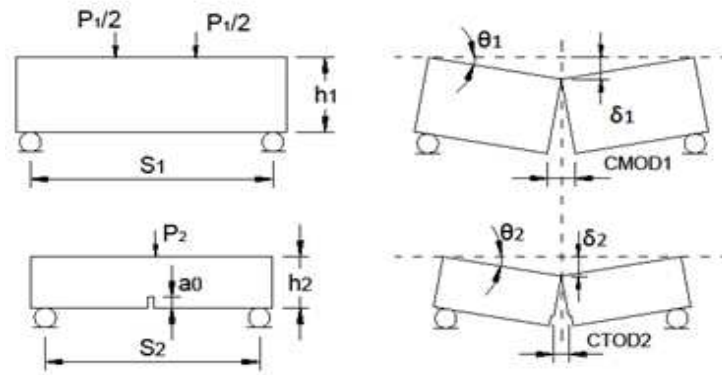
266

267 Where: A_{3mm} is the ratio of the area enveloped under the load-midspan deflection curve, from
268 the origin to the load at deflection equal to 3 mm. S is the span. B and h are the breadth (width)
269 and height of beam, respectively.

270

271 However, the beams used in this study were centrally notched, had dimensions of 80 (W) x
272 100 (H) x 400 (S) mm and were tested under the 3PB. In order to use the equivalent flexural
273 strength concept, which is defined at the specified deflection of 3 mm, it is necessary to
274 correlate the two different test methods via the relationship between deflection and CMOD.
275 In the post-peak region of a 3PB test, a hinge forms at the top of the beam, hence the residual
276 flexural strength is only dependent on the fibre reactions. For different dimensional beams
277 under bending test, the fibre effect can be regarded as similar if the crack lengths and crack
278 opening displacements of the two beams are identical. In order to compare the residual
279 strengths in the post-peak region measured from different geometrical beams, Giaccio et al.

280 [24] proposed an approach to determine the deflection limits of small beams to obtain design
 281 parameters of fibre-reinforced concrete.
 282 Consider the two types of beams with different dimensions under 4PB and 3PB shown in
 283 Figure 5. Beam one is the standard un-notched beam with the dimensions S_1 and h_1 under 4PB,
 284 while beam two is a centrally-notched beam with dimensions S_2 and h_2 and initial notch a_0
 285 under 3PB. In order to obtain identical fibre bridging effect, $CMOD_1$ should be equal to
 286 $CTOD_2$.
 287



288 **Figure 5.** Correlation of δ_1 and δ_2 of two beams with different dimensions

289
 290
 291 In the post-peak region, the relationships between deflection and the rotation angle and
 292 crack opening is as follows:

293
 294
$$\delta_1 = \theta_1 S_1 / 2 \tag{8}$$

295
$$\delta_2 = \theta_2 S_2 / 2 \tag{9}$$

296
$$CMOD_1 = 2h_1\theta_1 \tag{10}$$

297
$$CTOD_2 = 2(h_2 - a_0)\theta_2 \tag{11}$$

298

299 From the equations above and the condition of $CMOD_1 = CTOD_2$, the following equation is
300 obtained:

301

$$302 \quad \frac{\delta_1}{\delta_2} = \frac{s_1(h_2 - a_0)}{s_2 h_1} \quad (12)$$

303

304 The standard beam for testing equivalent flexural strength is 150 (W) x 150 (H) x 450 (S) mm,
305 and the specified deflection, $\delta_1 = 3$ mm. The beams used in this study were 80 (W) x 100 (H) x
306 400 (S) mm with an initial notch of 20 mm. Hence, substitution of these dimensions into eqn.
307 (12) results in:

308

$$309 \quad \delta_2 = 1.67 \delta_1 \quad (13)$$

310

311 Thus, the corresponding deflection limit, δ_2 , determined using eqn. (13) is 5 mm. Hereafter,
312 the equivalent strength for the deflection limit of 5 mm is denoted as $f_{e,5}$. The equivalent
313 flexural strengths $f_{e,5}$ are listed in Table 4.

314

315 **3.4 Standard Equivalent Flexural Strength, $f_{e,3}$**

316

317 However, the equivalent flexural strength, $f_{e,5}$, cannot be used directly for the design of the
318 SFRC overlay pavement proposed by Altoubat et al.[18], because specimen sizes affect the
319 flexural strength significantly. As has been presented earlier, the tested beams in this study
320 were of dimensions 80 (W) x 100 (H) x 400 (S) mm with a central notch of 20 mm, quite
321 different from the standard beam for testing equivalent flexural strength proposed by JSCE-

322 SF4 [22], which is of the dimensions 150 (W) x 150 (H) x 450 (S) mm. Therefore, the $f_{e,5}$
323 above needs to be converted by taking the size effect into account.

324 It is seen from Figure 4 that the flexural strength-CMOD curves for all mixes are basically
325 parallel to each other except for the mix PVAPMC1.5%-35. This indicates that all mixes have
326 the same scale factor for equivalent strength conversion. In order to use the SFRC pavement
327 design method proposed by Altoubat et al. [18], the $f_{e,5}$ has to be converted twice to obtain the
328 standard equivalent flexural strength, $f_{e,3}$.

329 First, it has to be converted from the 3PB to 4PB. Its conversion factor (β_1) has been
330 determined previously. Second, it has to be converted from a 4PB test with the beam of 100
331 mm height to a 4PB test with the standard beam of 150 mm height, via the conversion factor
332 (β_2) that can be determined using the size effect equation (6) for mix SBRPMC1.5%-35.

333 Both conversion factors are attributed to the size effect. Factor β_2 is for converting the strength
334 of the 'short' beam to that of the 'tall' beam, explained thoroughly by Bazant's theory [21].

335 The second conversion factor, β_2 , is calculated in the following way:

336

$$337 \quad \beta_2 = \frac{f_P \text{ (in 150mm-height beam)}}{f_P \text{ (in 100mm-height beam)}} = \frac{\sqrt{\frac{100}{2.7}-1}}{\sqrt{\frac{150}{2.7}-1}} = 0.813 \quad (14)$$

$$338 \quad \beta = \beta_1 \cdot \beta_2 \quad (15)$$

339 The process of calculating the total conversion factor β and the standard equivalent flexural
340 strength, $f_{e,3}$, are tabulated in Table 4. It is seen from Table 4 that the mix PVAPMC1.5%-35
341 developed the lowest standard equivalent flexural strength, although it exhibited very high
342 maximum flexural strength. The standard equivalent flexural strength, $f_{e,3}$ can be used for
343 SFR-RC-PMC overlay pavement design.

344

345

346

347 **Table 4**

348 Calculation of standard equivalent flexural strength $f_{3,e}$

Mix ID	$f_{e,5}$ (MPa)	f_p in 3PB (MPa)	f_p in 4PB (MPa)	First convers. factor β_1	Second convers. factor β_2	$f_{e,3}$ (MPa)
SBRPMC1%-35	8.87	12.24	N/A	0.823	0.813	5.93
SBRPMC1.5%-35	10.86	15.22	12.53	0.823	0.813	7.27
SBRPMC2%-35	14.05	17.05	N/A	0.823	0.813	9.4
Con.SBRPMC1.5%-35	9.13	10.37	9.49	0.915	0.813	6.79
SBRPMC1.5%-50	14.24	16.76	N/A	0.823	0.813	9.53
PVAPMC1.5%-35	10.05	16.6	13.2	0.795	0.813	6.49

349

350 **3.5 Verification.**

351

352 The experimental results of SBRPMC1.5%-35 beams with different notch lengths and beam
353 depths, which were previously used for establishing the size effect law, were reanalysed to
354 verify the method for calculating the equivalent flexural strength, $f_{e,3}$, which should be
355 theoretically identical. Two types of beams, i.e. three 80 (W) x 100 (H) x 400 (S) mm with 40
356 mm-long notch and two 100 (W) x 150 (H) x 500 (S) mm beams with 25 mm-long notch were
357 analysed. The deflection limit for the former, determined using eqn. (11), was 6.8 mm, while
358 that of the latter was 4 mm. The equivalent flexural strengths $f_{e,5}$, $f_{e,6.8}$ and $f_{e,4}$ corresponding
359 to the deflection limits of 5, 6.8 and 4 mm, and their conversion factors are tabulated in Table
360 5. It is seen that the standard equivalent flexural strengths, $f_{e,3}$, determined using the method
361 proposed are approximately identical. This validates the method for calculating the standard
362 equivalent flexural strength, $f_{e,3}$, for overlay pavement design.

363

364 **Table 5**

365 Standard equivalent flexural strength determined using experimental results of beams with different notch length
366 and beam depth (a_0 =notch length, h =height of beam)

Mix ID	a_0/h	$f_{e,5}/f_{e,6.8}/f_{e,4}$	f_p in 3PB	f_p in 4PB	β_1	β_2	$f_{e,3}$
	(mm/mm)	(MPa)	(MPa)	(MPa)			(MPa)
SBRPMC1.5%-35	20/100	10.86	15.22	12.53	0.823	0.813	7.27
	40/100	13.31	16.85	12.53	0.743	0.813	8.04
	25/150	8.89	11.94	N/A	0.823	1.00	7.32

367

368 4. Efficiency of Steel Fibre in Roller-Compacted Concrete.

369

370 Compared to conventional SFRCs, the SFR-RC-PMC has more air voids and relatively less
371 cement paste (Table 6), hence this may lead to:

- 372 a. The steel fibres may not be fully bonded by cement paste;
- 373 b. The steel fibres may be deformed during specimen formation due to compaction by
374 the vibrating compactor.

375 The two factors may consequently lead to poor steel fibre efficiency. In addition, the
376 efficiency of 50mm-long fibres also need to be quantitatively investigated by comparison with
377 35mm-long fibres. Steel fibres have been successfully used in conventional concrete to
378 improve the performance of concrete for several decades. The conventional concrete
379 containing the same steel fibre type and fibre content, can be a reliable benchmark for the
380 investigation of the fibre efficiency in SFR-RC-SBRPMC.

381 **Table 6** Table 6 shows the main physical parameters of the three mixes SBRPMC1.5%-35,
382 SBRPMC1.5%-50 and Con.SBRPMC1.5%-35. The mix Con.SBRPMC1.5%-35 was
383 conventional concrete, its slump of fresh mix was measured to be 130mm. The three mixes

384 contained the same fibre content and the beams were of the same dimensions to avoid any
 385 size effect.
 386 Table 6 clearly indicates that the water to cement ratios and cement paste contents of mixes
 387 SBRPMC1.5%-35 and SBRPMC1.5%-50 are much lower than those of the conventional
 388 Con.SBRPMC1.5%-35. Also, the former have higher air content than the latter.

389

390 **Table 6**

391 Comparison of physical properties of five mixes

Mix ID	Workability of fresh mixes	W/C	Cem. paste by volume (%)	Air content (%)
SBRPMC1.5%-35	Dry, non-slump	0.206	37.94	2.94
SBRPMC1.5%-50	Dry, non-slump	0.206	37.94	2.94
Con.SBRPMC1.5%-35	Wet, slump of 130mm	0.355	42.3	1.2
SBRPMC0%	Dry, non-slump	0.206	N/A	N/A
Con.SBRPMC0%	Wet, slump > 130mm	0.355	N/A	N/A

392 Note: the water for determining water to cement ratio and cement paste fraction included also the water

393 contained in SBR but excluded the water absorbed by the coarse aggregate.

394

395 The beam dimensions and test procedures for the three mixes SBRPMC1.5%-35,
 396 SBRPMC1.5%-50 and Con.SBRPMC1.5%-35 have been presented in Section 2 and Section
 397 3.1. The three mixes were tested under 3PB, and the experimental data have been analysed to
 398 evaluate maximum flexural strength, f_p , equivalent flexural strength, $f_{e,3}$, relative toughness
 399 index, I_t , defined as the ratio of fracture energy of SFRC to that of unreinforced concrete [27]
 400 and total fracture energy, G_F [23]. These mechanical parameters are rearranged to study the
 401 fibre efficiency in the following:

402 The total fracture energy was evaluated using the method recommended by the RILEM code
403 [25], i.e. it is equal to the work done by the externally applied load divided by the area of
404 fractured section of the beam.

405 The beams of mixes SBRPMC0% and Con.SBRPMC0% had midspan saw-cut notches to the
406 depth of 33 mm made prior to the test. The 3PB test was conducted to measure fracture
407 energy. The specimen dimensions and test procedure complied with the code of RILEM
408 Report 5 1991 [26]. However, the much lower than the recommended by the same code
409 CMOD - control loading rate was 0.0001 mm/s, in an effort to obtain stable load-deflection
410 curves. The test for each beam lasted about 30 minutes, longer than that recommended by the
411 RILEM code [26]. It is seen from Table 7 that:

- 412 a. The fibre in mix SBRPMC1.5%-35 exhibited much higher efficiency than the mix
413 Con.SBRPMC1.5%-35, indicating that the efficiency of fibres in these mixes is
414 much higher than that in conventional concrete.
- 415 b. The efficiency of fibres with aspect ratio of 80 in mix SBRPMC1.5%-50 was much
416 higher than the fibres with aspect ratio of 60 in SBRPMC1.5%-35, indicating the
417 fibre aspect ratio has remarkable influence on the flexural performance.

418

419 **Table 7**

420 Comparison of macro-mechanical properties of three mixes

Mix ID	f_p	$f_{e,3}$	G_F	I_t
	(MPa)	(MPa)	(J/m ²)	
SBRPMC1.5%-35	15.22	7.27	18580	221
SBRPMC1.5%-50	16.76	9.53	28300	337
Con.SBRPMC1.5%-35	10.37	6.79	15650	103

421

422 **5. Mechanism of Fibre Efficiency.**

423

424 Observations on SFRC beam under 3PB test indicated that the crack initiated from the notch
425 tip, and extended monotonically with load increments. The crack continued to extend but the
426 applied load begun to fall after the peak load was reached and a hinge formed beneath the top
427 of the beam. The complete process of failure of SFRC beam in flexure consisted of two stages:
428 At stage I, prior to hinge formation, the flexural performance mainly depends on the
429 interaction of matrix and fibres. At stage II, after the hinge formation, the flexural behaviour
430 depends mainly on the resistance induced by fibre traction. Therefore, it is reasonable to use
431 the relationship of fibre tensile stress and crack face opening displacement (fibre bridging law)
432 at stage-II to reveal the reasons why the efficiency of fibre in RCC was much higher than that
433 in conventional concrete. The fibre bridging at stage-II serves also as the fibre pull-out test.
434 Table 8 presents the fibre bridging law, for stage-II, for three mixes, established by using
435 inverse analysis presented in ref. [28] in detail. Figure 6 (b) provides a graphical
436 representation of the law for the same three mixes.

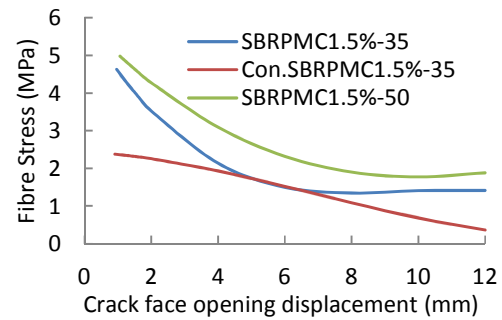
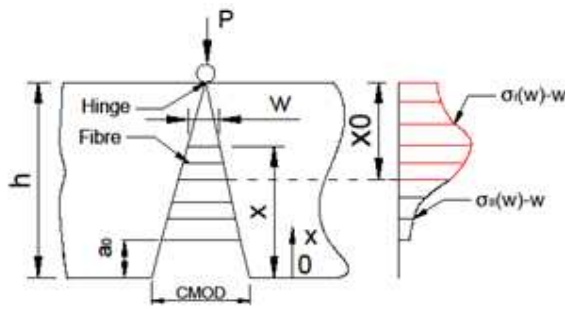
437

438 **Table 8**

439 Fibre bridging law for stage-II under 3BP [Units: σ (MPa), and w (mm)]

Mix ID	Fibre bridging law for stage-II under flexure
SBRPMC1.5%-35	$\sigma_{II}(w) = -0.0056w^3 + 0.1612w^2 - 1.5044w + 5.9306$ $0.958 \leq w \leq 12.45$
Con.SBRPMC1.5%-35	$\sigma_{II}(w) = 0.0012w^3 - 0.025w^2 - 0.0461w + 2.4392$ $0.907 \leq w \leq 12.64$
SBRPMC1.5%-50	$\sigma_{II}(w) = -0.0012w^3 + 0.0654w^2 - 0.9482w + 5.9164$ $1.063 \leq w \leq 12.99$

440



441

442

443

(a)

(b)

444

Figure. 6 (a) Fibre tensile stress after a hinge formation beneath the point load (a_0 =notch depth).

445

(b) Plots of fibre bridging laws in polynomial form as listed in Table 8

446

447

It is seen from Figure 6 (b) that both mixes SBRPMC1.5%-35 and Con.SBRPMC1.5%-35

448

contained the same amount and type of fibre, however the former exhibited higher tensile

449

strength than the latter, for a given face opening displacement. It is clear that the main

450

mechanism for the RCC having higher fibre efficiency than conventional concrete is

451

attributed to a lower water to cement ratio, resulting in higher friction between fibre and

452

mortar, although the air content of the former was higher than the latter. In addition, the curve

453

of fibre bridging law of SBRPMC1.5%-50 is above the curve of SBRPMC1.5%-35 at all

454

crack face opening displacements, implying that the former provided higher fibre traction.

455

The fibre bridging law can serve as an index to evaluate the fibre efficiency for the selection

456

of ingredients during the mix design process in practical (site) applications. For example,

457

mixes SBRPMC1.5%-35 and SBRPMC1.5%-50, in Table 8, are the same (have identical

458

proportions of ingredients), only the former incorporates shorter fibres than the latter. It is

459

apparent from Figure 6 (b) that SBRPMC1.5%-50 is more efficient than SBRPMC1.5%-35

460

because the fibres of mix -50 provide higher tensile strength than those of -35, for the same

461

crack opening displacement. In this case, the fibre bridging law specified in Table 8, can be

462

used to predict the flexural performance of beams made of the three different mixes.

463

464 **6. Concluding Remarks.**

465

466 1. Compared to conventional steel fibre-reinforced concrete, steel fibre- reinforced roller-
467 compacted polymer modified concrete developed very high flexural strength. This is
468 very favourable to worn concrete pavement rehabilitation.

469 2. The standard equivalent flexural strengths evaluated using the method proposed by this
470 study are listed in Table 4, and can be directly used for overlay pavement design. The
471 method, using the identical fibre bridging concept and size effect, has been verified
472 successfully.

473 3. Mix SBRPMC1.5%-35 is deemed to be optimum for both, strength and workability.
474 Mix PVAPMC1.5%-35 exhibited higher flexural and bond strength with the old
475 concrete than mix SBRPMC1.5%-35 but unfortunately low equivalent flexural strength
476 which is the basis of overlay design and thus is not a suitable mix for worn concrete
477 pavement rehabilitation.

478 4. The fibres in SFR-RC-PMC exhibited much higher efficiency than in conventional
479 SFRC (consolidated by vibrating table). This is mainly attributed to a lower water to
480 cement ratio. This indicates that these mixes are economically viable.

481

482 **Acknowledgements**

483

484 The financial support of the Engineering and Physical Sciences Research Council (EPSRC, Ind. Case
485 Studentship, No. 08002550), and Aggregate Industries, UK, is gratefully acknowledged. The authors would like
486 to express their gratitude to their colleague, Ms. Yi Xu, for her help during lab work; and to Mr. Ian Breakwell,
487 senior technician at the Civil Engineering Laboratories, Coventry University for his valuable suggestions,
488 comments and help. Special mention should also be made of Tarmac, AGS Mineraux, Power Minerals and
489 Nippon Gohsei EU for providing materials for research.

490

491 **References**

492

- 493 [1] Lin, Y.; Karadelis, J.N.; Xu, Y. A new mix design method for steel fibre-reinforced, roller
494 compacted and polymer modified bonded concrete overlays, *Construction and Building*
495 *Materials*, 48 (2013) 333 – 341.
- 496 [2] ASTM C 1170-06. Standard test method for determining consistency and density of roller-
497 compacted concrete using a vibrating table, *ASTM Committee C09*, 2006, USA.
- 498 [3] ACI Committee 207. Roller-Compacted Mass Concrete (ACI 207.5R-99), 1999, ACI, USA.
- 499 [4] Jenq, Y. S.; Shah, S. P. Crack propagation in fibre-reinforced concrete, *Journal of Structural*
500 *Engineering*, 1986, Vol.112, No.1, 19 – 34.
- 501 [5] Gopalaratnam, V. S.; Shah, S. P.; Batson, G. B.; Criswell, M. E.; Ramakrishnan, V.;
502 Wecharatana, M. Fracture toughness of fibre reinforced concrete, *ACI Materials Journal*, Vol.
503 88, No. 4, 1991, 339 - 353.
- 504 [6] Banthia, N.; Trottier, J.F. Test method for flexural toughness characterization of fibre reinforced
505 concrete: some concerns and a proposition, *ACI Materials Journal*, Vol. 92, No.1, 1995a, 48-57.
- 506 [7] Banthia, N.; Trottier, J.F.; Concrete reinforced with deformed steel fibres Part II: Toughness
507 characterization, *ACI Materials Journal*, Vol. 92, No. 2, 1995b, 146 - 154.
- 508 [8] Armelin, H.S.; Banthia, N. Predicting the flexural post-cracking performance of steel fibre
509 reinforced concrete from the pullout of single fibres, *ACI Materials Journal*, V.94, No.1,
510 January- February, 1997, pp.18 - 31.
- 511 [9] Lok, T. S.; Pei, J. S. Flexural behaviour of steel fibre reinforced concrete, *Journal of Materials*
512 *in Civil Engineering*, Vol. 10, No. 2, 1998, 86 - 97.
- 513 [10] Jeng, F.; Lin, M.L.; Yuan, S.C.; Performance of toughness indices for steel fibre reinforced
514 shotcrete, *Tunnelling and underground space technology*, 17 (2002), 69-82.
- 515 [11] Denneman, E.; Wu, R.; Kearsley, E.P.; Visser, A.T. Discrete fracture in high performance fibre
516 reinforced concrete materials, *Engineering Fracture Mechanics*, 78 (2011), 2235-2245.
- 517 [12] Neocleous, K.; Angelakopoulos, H.; Pilakoutas, K.; Guadagnini, M. Fibre-reinforced roller-
518 compacted concrete transport pavements, *Proceedings of the Institution of Civil Engineers, UK,*
519 *Transport 164*, May 2011 Issue TR2.,97-109.
- 520 [13] Neocleous, K.; Tlemat, H.; Pilakoutas, K. Design issues for concrete reinforced with steel fibres,
521 including fibres recovered from used tires, *Journal of Materials in Civil Engineering*, V. 18, N.
522 5, 2006, 677-685.
- 523 [14] Kagaya, M.; Suzuki, T.; Kokubun, S.; Tokuda, H.; 2001, A study on mix proportions and
524 properties of steel fibre reinforced roller-compacted concrete for pavements, (*Translation from*
525 *Proceedings of JSCE*, No.669/V-50, February 2001).
- 526 [15] British Standard BS EN14651:2005+A1: 2007, Test method for metallic fibre concrete —
527 Measuring the flexural tensile strength (limit of proportionality (LOP), residual), British
528 Standard Institution, UK.
- 529 [16] ASTM C 1609/C 1609M-06 Standard Test Method for Flexural Performance of Fibre-
530 Reinforced Concrete (Using Beam with Three-Point Loading), *ASTM International*, 2006, USA.
- 531 [17] Lin, Y.; Karadelis, J.N. Strain energy release rate at interface of concrete overlay pavements,
532 *International Journal of Pavement Engineering*, 2014 (under review).
- 533 [18] Altoubat, S.A; Roesler, J.R.; Lange, D.A.; Rieder, K. A. Simplified method for concrete
534 pavement design with discrete structural fibres, *Construction and Building Materials*, 22 (2008),
535 384-393.
- 536 [19] Quinn, G.D. Weibull strength scaling for standardized rectangular flexure specimens. *Journal of*
537 *American Ceramics Society*, 2003, 86:508-10.
- 538 [20] Bazant, Z.P.; 1984, Size effect in blunt fracture: concrete, rock, metal. *Journal of Engineering*
539 *Mechanics*, Vol. 81, No. 5, pp. 456-468.

- 540 [21] Bazant, Z.P. Fracture energy of heterogeneous materials and similitude in Fracture of Concrete
541 and Rock, edited by Shah, S.P., and Swartz, S.E., Pringer-Verlag, New York, 1989, 229-241.
- 542 [22] Japan Society of Civil Engineers JSCE-SF4. Methods of tests for flexural strength and flexural
543 toughness of steel fibre reinforced concrete, *Concrete Library International*, Part III-2, No.3;
544 1984, 58-61.
- 545 [23] Lin, Y. Optimum Design for Sustainable ‘Green’ Bonded Concrete Overlays: Controlling
546 Flexural Failure. PhD Thesis, Department of Civil Engineering, Architecture and Building,
547 Faculty of Engineering and Computing, Coventry University, 2014, UK. (unpublished)
- 548 [24] Giaccio, G.; Tobes, J. M.; Zerbino, R. Use of small beams to obtain design parameters of fibre
549 reinforced concrete, *Cement and Concrete Composites*, v 30, n 4, 2008, 297-306.
- 550 [25] RILEM, Committee on Fracture mechanics of concrete. Test methods: Determination of the
551 fracture energy of mortar and concrete by means of three-point bend test on notched beams,
552 *Materials and Structures*, Vol.10, No.106, 1985, 285-290.
- 553 [26] RILEM, Fracture mechanics test method for concrete, Report 5, 89-FMT, Shah, S.P. and
554 Carpinteri, A (Eds). 1991.
- 555 [27] ACI Committee 544.2R-89, 1988, Reapproved in 2009, Measurement of properties of fibre-
556 reinforced concrete.
- 557 [28] Lin, Y.; Karadelis, J.N. 2014 On Establishing the Fibre Bridging Law by an Inverse Analysis
558 Approach, *ASCE Journal of Materials in Civil Engineering*, (under review).
559